Am J Transl Res 2017;9(7):3167-3183
www.ajtr.org /ISSN:1943-8141/AJTR0053169

*Original Article*

# Exendin-4-assisted adipose derived mesenchymal stem cell therapy protects renal function against co-existing acute kidney ischemia-reperfusion injury and severe sepsis syndrome in rat

Pei-Hsun Sung[1*], Hsin-Ju Chiang[2,3*], Christopher Glenn Wallace[4], Chih-Chao Yang[5], Yen-Ta Chen[6], Kuan-Hung Chen[7], Chih-Hung Chen[8], Pei-Lin Shao[9], Yung-Lung Chen[1], Sarah Chua[1], Han-Tan Chai[1], Yi-Ling Chen[1], Tien-Hung Huang[1], Hon-Kan Yip[1,9,10,11,12], Mel S Lee[13]

*[1]Division of Cardiology, Department of Internal Medicine, Chang Gung Memorial Hospital and Chang Gung University College of Medicine, Kaohsiung, Taiwan, R.O.C.; [2]Department of Obstetrics and Gynecology, Kaohsiung Chang Gung Memorial Hospital and Chang Gung University College of Medicine, Kaohsiung, Taiwan, R.O.C.; [3]Chung Shan Medical University School of Medicine, Taichung, Taiwan, R.O.C.; [4]Department of Plastic Surgery, University Hospital of South Manchester, Manchester, UK; [5]Division of Nephrology, Department of Internal Medicine, Kaohsiung Chang Gung Memorial Hospital and Chang Gung University College of Medicine, Kaohsiung, Taiwan, R.O.C.; [6]Division of Urology, Department of Surgery, Kaohsiung Chang Gung Memorial Hospital and Chang Gung University College of Medicine, Kaohsiung, Taiwan, R.O.C.; [7]Department of Anesthesiology, Kaohsiung Chang Gung Memorial Hospital and Chang Gung University College of Medicine, Kaohsiung, Taiwan, R.O.C.; [8]Division of General Medicine, Department of Internal Medicine, Kaohsiung Chang Gung Memorial Hospital and Chang Gung University College of Medicine, Kaohsiung, Taiwan, R.O.C.; [9]Department of Nursing, Asia University, Taichung, Taiwan, R.O.C.; [10]Institute for Translational Research in Biomedicine, Kaohsiung Chang Gung Memorial Hospital, Kaohsiung, Taiwan, R.O.C.; [11]Center for Shockwave Medicine and Tissue Engineering, Kaohsiung Chang Gung Memorial Hospital, Kaohsiung, Taiwan, R.O.C.; [12]Department of Medical Research, China Medical University Hospital, China Medical University, Taichung, Taiwan, R.O.C.; [13]Department of Orthopedics, Kaohsiung Chang Gung Memorial Hospital, College of Medicine, Chang Gung University, Kaohsiung, Taiwan, R.O.C. [*]Equal contributors.*

Received March 17, 2017; Accepted June 6, 2017; Epub July 15, 2017; Published July 30, 2017

**Abstract:** This study tested the hypothesis that combined therapy with exendin-4 (Ex4) and autologous adipose-derived mesenchymal stem cells (ADMSCs) was superior to either alone for protecting renal function against acute kidney ischemia-reperfusion (IR; 40-min ischemia/27-h reperfusion) injury when complicated by sepsis syndrome (SS; by cecal-ligation-puncture). Adult-male Sprague-Dawley rats (n=40) were equally divided into group 1 (sham-control), group 2 (IR-SS), group 3 (IR-SS + Ex4, 10 μg/kg subcutaneously 30 min after reperfusion and daily for 3 days), group 4 [IR-SS + ADMSC ($1.2 \times 10^6$)], and group 5 (IR-SS + Ex4 + ADMSC). The circulating levels of BUN and creatinine and the ratio of urine protein to creatinine were highest in group 2, lowest in group 1, significantly higher in groups 3 and 4 than group 5, and significantly higher in group 3 than in group 4 (all P<0.0001). Microscopic findings of kidney injury score, inflammatory cells (CD14+, F4/80+), and expressions of glomerular-damage indicators (FSP-1+/WT-1+) and renal tubular-damage indicators (KIM-1+/snail+) showed an identical pattern, whereas expressions of indices of glomerular-integrity (ZO-1+/p-cadherin+/podocin+/synaptopodin+) and angiogenesis (CD31+/vWF+/number of small vessels) biomarkers demonstrated an opposite pattern, to that of creatinine level (all P<0.001). Protein expressions of inflammatory (MMP-9/IL-1ß/TNF-α/TLR-2/TLR-4), apoptotic (cleaved caspase-3/PARP/mitochondrial Bax), and oxidative-stress (NOX-1/NOX-2/oxidized protein) biomarkers exhibited an identical pattern, whereas anti-inflammatory (IL-10/IL-4) biomarkers displayed an opposite pattern, to that of creatinine level (all P<0.001). In conclusion, combined Ex4 and ADMSC therapy significantly protected kidney from acute IR-SS injury.

**Keywords:** Ischemia-reperfusion injury, sepsis syndrome, exendin-4, adipose derived mesenchymal stem cells, oxidative stress

## Introduction

Acute kidney injury (AKI) is a common, heterogeneous clinical syndrome encompassing a spectrum of risk factors, etiologies and precipitatory acute insults, which occurs in multiple settings, including acute ischemia-reperfusion (IR) injury [1-4]. AKI can be classified according

to the RIFLE (Risk, Injury, Failure, Loss and End-stage) and/or the Acute Kidney Injury Network (AKIN) criteria [5, 6]. Acute IR injury is one of the most common etiologies referred to within the Injury domain of the RIFLE classification and AKI is commonly caused by severe septic shock [6-9]. Previous studies have revealed that acute kidney IR injury complicated by severe sepsis is the leading cause of hospitalization for AKI and is associated with high morbidity and mortality [6-9], especially in patients who are immunocompromised, elderly or have diabetes mellitus (DM). There is currently no accepted effective treatment for acute kidney IR injury/AKI complicated by severe sepsis with septic shock.

Consistent with other causes of sepsis syndrome, acute kidney IR injury/AKI complicated by severe sepsis triggers a variety of inflammatory changes, culminating an overwhelming host immune response. This enhances the generation of oxidative stress and reactive oxygen species (ROS), increases the metabolic and humoral pathways and leads to remote organ dysfunction with detrimental effects on both short and long-term outcomes [9-13].

Exendin-4 (Ex4), a glucagon-like peptide-1 (GLP-1) analogue, was originally used to treat type 2 DM patients. Copious data have displayed that Ex4 therapy has protective effects against ischemia-induced tissue and organ damage mainly via its anti-oxidative and anti-inflammatory properties [14-17]; these are in addition to its hypoglycemic function [14-19]. Our recent studies have also shown that Ex4 possesses anti-apoptotic, anti-oxidative and anti-fibrotic capacity in the setting of ischemia-reperfusion organ injury [15] and ischemia-related organ dysfunction [14, 16, 17]. Plentiful investigations have shown that cell-based therapy provides a new therapeutic modality for ischemia-related organ dysfunction refractory to conventional therapy. Mesenchymal stem cells (MSC), particularly adipose-derived MSCs (ADMSCs), have immunomodulatory capacity and can suppress inflammation and oxidative stress [20-24]. We recently reported that ADMSC therapy effectively reduced acute urogenital organ damage and mortality rate in rat sepsis syndrome [13]. Accordingly, this study, tested the hypothesis that Ex4-assisted ADMSC therapy might be superior to either one alone for preserving kidney function in the setting of acute kidney IR injury complicated by sepsis syndrome (SS).

## Materials and methods

### *Ethics*

Both animal experimental protocols and procedures were approved by our Institute of Animal Care and Use Committee at Kaohsiung Chang Gung Memorial Hospital (Affidavit of Approval of Animal Use Protocol No. 2015032502) and executed in accordance with the Guide for the Care and Use of Laboratory Animals [The Eighth Edition of the Guide for the Care and Use of Laboratory Animals (NRC 2011)].

Animals were housed in an Association for Assessment and Accreditation of Laboratory Animal Care International (AAALAC)-approved animal facility in our hospital with controlled temperature and light cycles (24°C and 12/12 light cycles).

### *Procedure and protocol of acute kidney ischemia-reperfusion (IR)*

Pathogen-free, adult male Sprague-Dawley (SD) rats (n=40) weighing 320-350 g (Charles River Technology, BioLASCO Taiwan Co. Ltd., Taiwan) were utilized in the present study. The protocol for the acute kidney IR procedure has been detailed in our previous reports [15, 17, 23]. Briefly, animals were anesthetized by inhalational 2.0% isoflurane and placed supine on a warming pad at 37°C for midline laparotomies. The sham control (SC) animals underwent laparotomy only. Acute IR injury of both kidneys was induced in all animals in acute kidney IR groups by clamping the renal pedicles for 40 minutes using non-traumatic vascular clips.

### *Procedure for SS induction by cecal ligation and puncture (CLP)*

The procedure and protocol for SS induction, which was performed immediately after acute kidney IR procedure, was based on our previous report [24]. In the experimental CLP groups, the cecum of each animal was prolene suture-ligated at its distal portion (i.e. distal ligation), the cecum distal to the ligature was punctured twice with an 18G needle, and the distal cecal contents were manually expressed intraperitoneally. The abdominal muscle and skin were sutured and the animal was allowed to recover from anesthesia.

The animals in each group were euthanized and kidney specimens were collected for individual study by day 3 after the IR procedure.

*Animal grouping and rationale for the therapeutic regimen*

The animals were equally categorized into five groups (i.e., n=8/each group): Sham control (SC; laparotomy plus intra-peritoneal administration of 3.0 mL normal saline at 30 minutes and days 1 to 3 after IR procedure), IR-SS (receiving the same treatment as SC except for IR of both kidneys and SS induction), IR-SS + exendin-4 [(IR-SS + Ex4), subcutaneous administration of exendin-4 10 μg/kg at 30 minutes and at days 1 to 3 after IR procedure], IR-SS + ADMSC ($1.2 \times 10^6$ cells intravenous administration at 3 h after IR procedure), and IR-SS + Ex4 + ADMSC.

The dosages and timings for exendin-4 administration were based on our recent reports [15-17]. The dosages and timings for ADMSC administration were based on our recent reports [13, 20, 21, 23-25].

*Flow cytometric analysis of circulatory inflammatory biomarkers day 3 after acute kidney IR-SS procedure*

*Whole blood-derived Ly6G (lymphocyte antigen 6 complex locus G6D):* Population of Ly6G positive cells from whole blood was determined by CytomicsTM FC500 flow cytometer (BD Biosciences, California, USA). Briefly, whole blood was diluted by PBS and further incubated with anti-rat Ly6G-FITC antibody for 30 minutes at room temperature. Incubated cells were washed with RBC lysis buffer (155 mM $NH_4Cl$, 12 mM $NaHCO_3$, 0.1 mM EDTA, in 1 L di-water, pH7.3) for 5 minutes and re-suspend in PBS for analysis. The results were recorded and evaluated by the CXP Analysis software (BD Biosciences, California, USA).

*Peripheral blood mononuclear cell (PBMCs)-derived CD12/TLR2 CD12/TLR4:* Population of toll-like receptor (TLR)-2, TLR-4, CD12/TLR2 and CD12/TLR4 positive cells were determined by (BD Biosciences, California, USA). Briefly, PBMCs were isolated by applying the Ficoll-Plaque density gradient centrifugation and further washed by PBS for 5 minutes twice. PBMCs were re-suspend in PBS and incubated with antibodies for 40 minutes at room temperature, antibodies including anti-rat CD14-FITC (Biobyte), anti-rat TLR2-PE (abcam), and anti-rat TLR4-PE (abcam). Incubated PBMCs were then washed by PBS for 5 minutes and were subjected to analyze. The results were recorded and evaluated by the CXP Analysis software (BD Biosciences, California, USA).

*Determining serum creatinine and BUN levels, and collection of 24-hour urine for the ratio of urine protein to creatinine at baseline and day 3 after acute kidney IR-SS procedure*

Blood samples were collected from all animals in each group to measure changes in serum creatinine and blood urine nitrogen (BUN) levels prior to and at 72 h after IR procedure.

For the collection of 24-hr urine for individual study, each animal was placed into a metabolic cage [DXL-D, space: 190 × 290 × 550, Suzhou Fengshi Laboratory Animal Equipment Co. Ltd., Mainland China] for 24 hrs with free access to food and water. Urine in 24 hrs was collected in all animals prior to and at 72 h after the IR procedure to determine the daily urine volume and the ratio of urine protein to urine creatinine.

*Kidney injury scores at day 3 after acute kidney IR-SS procedure*

Histopathology scoring was assessed in a blinded fashion as we have previously described [15, 23, 25]. Briefly, the kidney specimens from all animals were fixed in 10% buffered formalin, embedded in paraffin, sectioned at 5 μm and stained with hematoxylin and eosin (H&E) for light microscopy. The scoring system reflects the grading of tubular necrosis, loss of brush border, cast formation, and tubular dilatation in 10 randomly chosen, non-overlapping fields (200 x) as follows: 0 (none), 1 (≤10%), 2 (11-25%), 3 (26-45%), 4 (46-75%), and 5 (≥76%) [23].

*Immunohistochemical (IHC) and immunofluorescent (IF) staining*

The procedure and protocol for IHC and IF staining have previously been reported in detail [13-17, 20, 21, 23-25]. For IHC and IF staining, rehydrated paraffin sections were first treated with 3% $H_2O_2$ for 30 minutes and incubated with Immuno-Block reagent (BioSB, Santa Barbara, CA, USA) for 30 minutes at room temperature. Sections were then incubated with primary antibodies specifically against zonula occludens-1 (ZO-1) (1:300, Abcam, Cambridge, MA,

USA), Wilm's tumor suppressor gene 1 (WT-1) (1:1000, Abcam, Cambridge, MA, USA), kidney injury molecule (KIM)-1 (1:200, R&D system, Minneapolis, MN, USA), fibroblast specific protein (FSP)-1 (1:200, Abcam, Cambridge, MA, USA), P-cadherin (1:100, Novus, Littleton, CO, USA), snail (1:300, Abcam, Cambridge, MA, USA), podocin (1:100, Sigma, St. Louis, Mo, USA), dystrophin (1:100, Abcam, Cambridge, MA, USA), fibronectin (1:200, Abcam, Cambridge, MA, USA), and synaptopodin (1:100, Santa Cruz, Santa Cruze, CA, USA) while sections incubated with irrelevant antibodies served as controls. Three kidney sections from each rat were analyzed. For quantification, three randomly selected HPFs (200 x for IHC; 400 x for IF) were analyzed in each section. The mean number of positively-stained cells per HPF for each animal was then determined by summation of all numbers divided by 9.

An IHC/IF-based scoring system was adopted for semi-quantitative analyses of KIM-1, ZO-1, podocin, SFP-1, synaptopodin, snail and WT-1 as percentage of positive cells in a blind fashion [Score of positively-stained cell for podocin and WT-1: 0= no stain %; 1≤15%; 2=15~25%; 3=25~50%; 4=50~75%; 5≥75%-100%/per high-power filed (400 x)].

*Western blot analysis*

The procedure and protocol for Western blot analysis have been described in our previous reports [13-17, 20, 21, 23-25]. Briefly, equal amounts (50 μg) of protein extract were loaded and separated by SDS-PAGE using acrylamide gradients. After electrophoresis, the separated proteins were transferred electrophoretically to a polyvinylidene difluoride (PVDF) membrane (Amersham Biosciences, Amersham, UK). Nonspecific sites were blocked by incubation of the membrane in blocking buffer [5% nonfat dry milk in T-TBS (TBS containing 0.05% Tween 20)] overnight. The membranes were incubated with the indicated primary antibodies [matrix metalloproteinase (MMP)-9 (1:3000, Abcam, Cambridge, MA, USA), tumor necrosis factor (TNF)-α (1:1000, Cell Signaling, Danvers, MA, USA), nuclear factor (NF)-κB (1:600, Abcam, Cambridge, MA, USA), NADPH oxidase (NOX)-1 (1:1500, Sigma, St. Louis, Mo, USA), NOX-2 (1:750, Sigma, St. Louis, Mo, USA), and actin (1:10000, Chemicon, Billerica, MA, USA)] for 1 hour at room temperature. Horseradish peroxidase-conjugated anti-rabbit immunoglobulin IgG (1:2000, Cell Signaling, Danvers, MA, USA) was used as a secondary antibody for one-hour incubation at room temperature. The washing procedure was repeated eight times within one hour. Immunoreactive bands were visualized by enhanced chemiluminescence (ECL; Amersham Biosciences, Amersham, UK) and exposed to Biomax L film (Kodak, Rochester, NY, USA). For quantification, ECL signals were digitized using Labwork software (UVP, Waltham, MA, USA).

*Assessment of oxidative stress*

The procedure and protocol for assessing the protein expression of oxidative stress have been detailed in our previous reports [13-17, 20, 21, 23-25]. The Oxyblot Oxidized Protein Detection Kit was purchased from Chemicon, Billerica, MA, USA (S7150). DNPH derivatization was carried out on 6 μg of protein for 15 minutes according to the manufacturer's instructions. One-dimensional electrophoresis was carried out on 12% SDS/polyacrylamide gel after DNPH derivatization. Proteins were transferred to nitrocellulose membranes which were then incubated in the primary antibody solution (anti-DNP 1:150) for 2 hours, followed by incubation in secondary antibody solution (1:300) for 1 hour at room temperature. The washing procedure was repeated eight times within 40 minutes. Immunoreactive bands were visualized by enhanced chemiluminescence (ECL; Amersham Biosciences, Amersham, UK) which was then exposed to Biomax L film (Kodak, Rochester, NY, USA). For quantification, ECL signals were digitized using Labwork software (UVP, Waltham, MA, USA). For Oxyblot protein analysis, a standard control was loaded on each gel.

*Statistical analysis*

Quantitative data are expressed as means ± SD. Statistical analysis was adequately performed by ANOVA followed by Bonferroni multiple-comparison post hoc test. Statistical analysis was performed using SPSS statistical software for Windows version 13 (SPSS for Windows, version 13; SPSS, IL, U.S.A.). A *P* value of less than 0.05 was considered statistically significant.

## Results

*Creatinine and BUN levels, urine amount and the ratio of urine protein to creatinine at baseline and day 3 after IR-SS procedure (**Figure 1**)*

Prior to the IR-SS procedure, the circulating levels of creatinine and BUN, urine volume, and

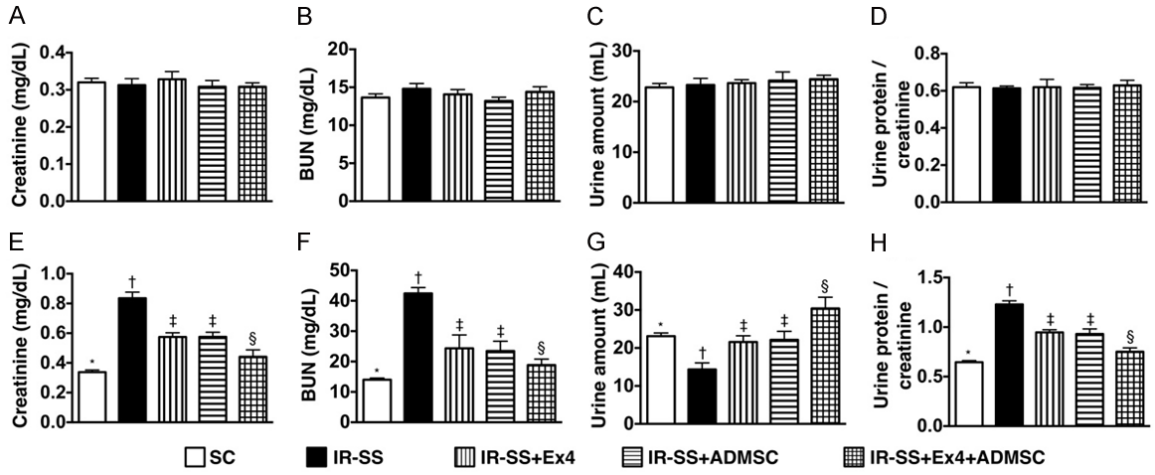


**Figure 1.** Circulating levels of creatinine, blood urine nitrogen (BUN), urine amount, and the ratio of urine protein to creatinine at baseline and day 3 after IR-SS procedure. By day 0 prior to IR-SS procedure: A. Creatinine level, SC vs. other groups, P>0.5. B. BUN level, SC vs. other groups, P>0.5. C. Urine amount, SC vs. other groups, P>0.5. D. Ratio of urine protein to creatinine, SC vs. other groups, P>0.5. By day 3 after IR-SS procedure: E. Creatinine level, * vs. other groups with different symbols (†, ‡, §), P<0.0001. F. BUN level, * vs. other groups with different symbols (†, ‡, §), P<0.0001. G. Urine amount, * vs. other groups with different symbols (†, ‡, §), P<0.0001. H. Ratio of urine protein to creatinine, * vs. other groups with different symbols (†, ‡, §), P<0.0001. All statistical analyses were performed by one-way ANOVA, followed by Bonferroni multiple comparison post hoc test (at least n=7 for each group). Symbols (*, †, ‡, §) indicate significance at the 0.05 level. SC = sham-operative control; IR-SS = ischemia-reperfusion and sepsis syndrome; Ex4 = exendin-4; ADMSC = adipose-derived mesenchymal stem cell.

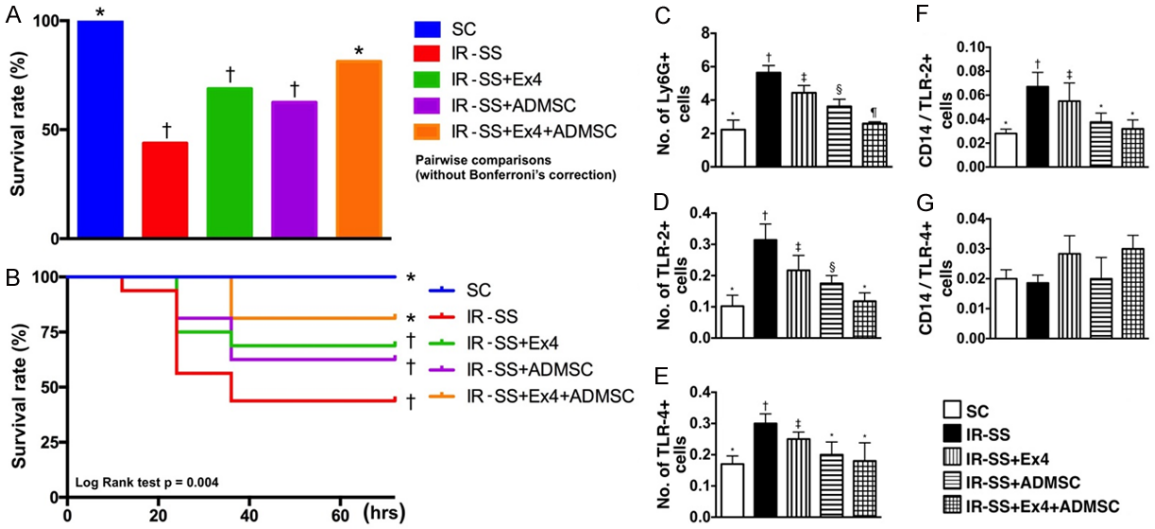


**Figure 2.** Flow cytometric assessment of circulating inflammatory biomarkers and mortality rate by day 3 after IR-SS procedure. A. The survival rate of five groups (n=16) by rate Pairwise comparisons (without Bonferroni's correction), * vs. †, P<0.0005. B. Kaplan Meier survival cure. By log Rank test, P=0.004. C. Circulating number of Ly6G+ cells, * vs. other groups with different symbols (†, ‡, §, ¶), P<0.0001. D. Circulating number of tall-like receptor (TLR)-2+ cells, * vs. other groups with different symbols (†, ‡, §), P<0.001. E. Circulating number of TLR-4+ cells, * vs. other groups with different symbols (†, ‡), P<0.001. F. Circulating level of CD14/TLR-2+ cells (i.e., double stain), * vs. other groups with different symbols (†, ‡), P<0.001. G. Circulating number of CD14/TLR-4+ cells (double stain) did not differ among the five groups, P>0.2. All statistical analyses were performed by one-way ANOVA, followed by Bonferroni multiple comparison post hoc test (at least n=7 for each group). Symbols (*, †, ‡, §) indicate significance at the 0.05 level. SC = sham-operative control; IR-SS = ischemia-reperfusion and sepsis syndrome; Ex4 = exendin-4; ADMSC = adipose-derived mesenchymal stem cell.

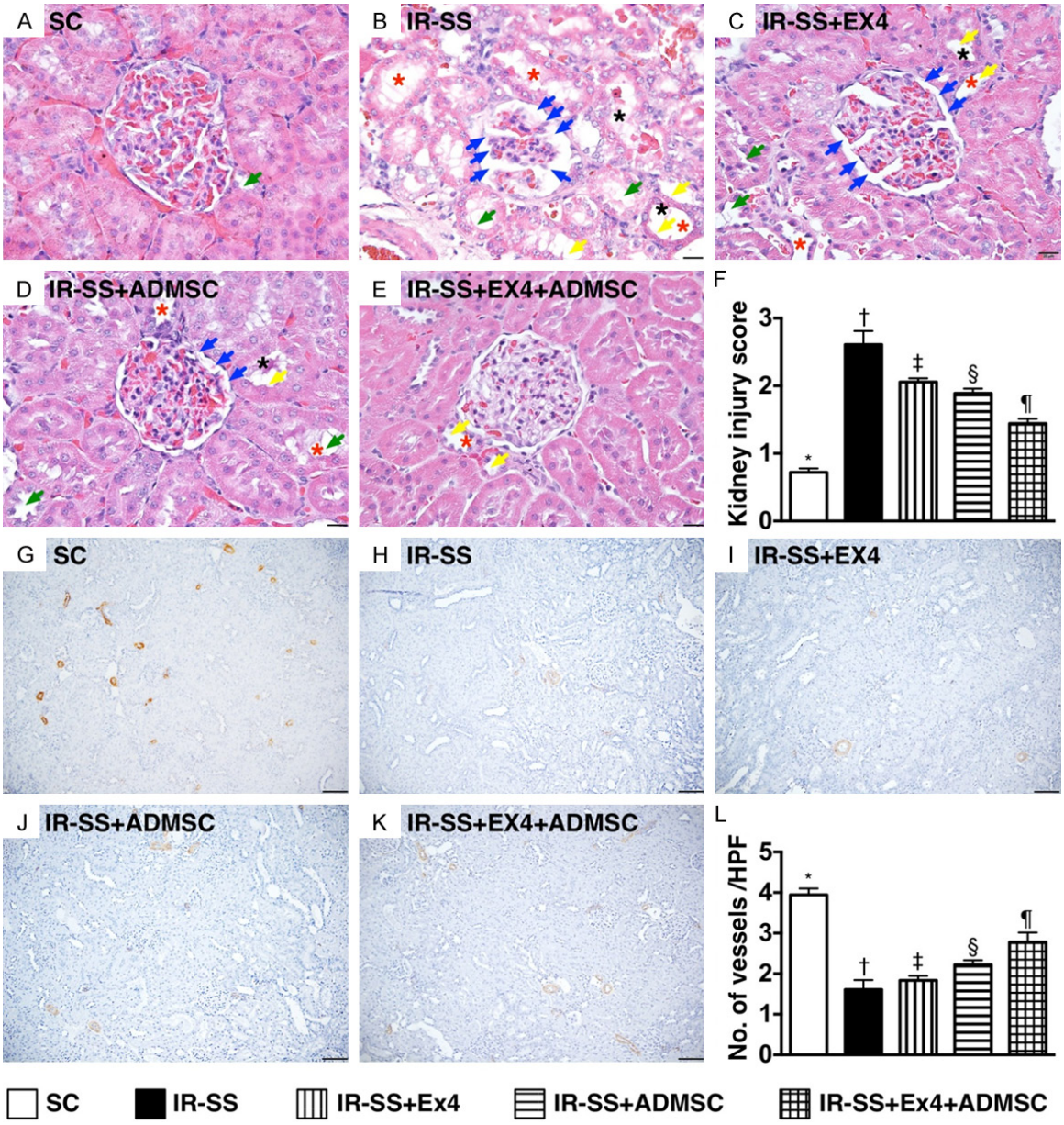


**Figure 3.** Histopathological findings of kidney injury score and small vessel density in kidney parenchyma by day 3 after IR-SS procedure. A-E. Light microscopic findings of H&E. stain (400 x) demonstrating significantly higher degree of loss of brush border in renal tubules (yellow arrows), tubular necrosis (green arrows), tubular dilatation (red asterisk), protein cast formation (black asterisk), and dilatation of Bowman's capsule (blue arrows) in IR group than in other groups. F. * vs. other groups with different symbols (†, ‡, §, ¶), P<0.0001. Scale bars in right lower corner represent 20 μm. G-K. Microscopy (100 x) for α-smooth muscle actin staining to identify the number of small vessels (red color; i.e. diameter ≤25 μM) in kidney parenchyma. L. Analytical results of number of small vessel, * vs. other groups with different symbols (†, ‡, §, ¶), P<0.0001. Scale bars in right lower corner represent 100 μm. All statistical analyses were performed by one-way ANOVA, followed by Bonferroni multiple comparison post hoc test (at least n=7 for each group). Symbols (*, †, ‡, §, ¶) indicate significance (at 0.05 level). SC = sham-operative control; IR-SS = ischemia-reperfusion and sepsis syndrome; Ex4 = exendin-4; ADMSC = adipose-derived mesenchymal stem cell.

the ratio of urine protein to urine creatinine did not differ among the five groups (**Figure 1A-D**). However, by 72 h after IR-SS procedure, the creatinine and BUN levels, two indicators of renal dysfunction (**Figure 1E**, **1F**), and the ratio of urine protein to urine creatinine, an indicator

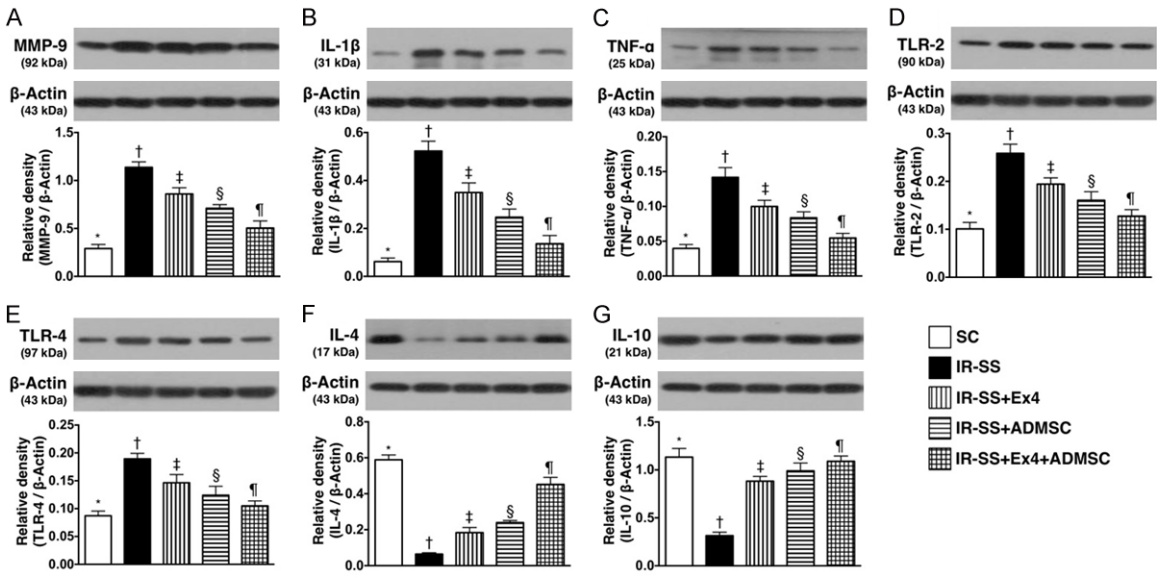


**Figure 4.** Protein expressions of inflammatory and anti-inflammatory biomarkers in kidney parenchyma by day 3 after IR-SS procedure. A. Protein expression of matrix metalloproteinase (MMP)-9, * vs. other groups with different symbols (†, ‡, §, ¶), P<0.0001. B. Protein expression of interleukin (IL)-1ß, * vs. other groups with different symbols (†, ‡, §, ¶), P<0.0001. C. Protein expression of tumor necrosis factor (TNF)-α, * vs. other groups with different symbols (†, ‡, §, ¶), p<0.0001. D. Protein expression of toll-like receptor (TLR)-2, * vs. other groups with different symbols (†, ‡, §, ¶), P<0.0001. E. Protein expression of TLR-4, * vs. other groups with different symbols (†, ‡, §, ¶), P<0.0001. F. Protein expression of IL-4, * vs. other groups with different symbols (†, ‡, §, ¶), P<0.0001. G. Protein expression of IL-10, * vs. other groups with different symbols (†, ‡, §, ¶), P<0.0001. All statistical analyses were performed by one-way ANOVA, followed by Bonferroni multiple comparison post hoc test (at least n=7 for each group). Symbols (*, †, ‡, §, ¶) indicate significance (at 0.05 level). SC = sham-operative control; IR-SS = ischemia-reperfusion and sepsis syndrome; Ex4 = exendin-4; ADMSC = adipose-derived mesenchymal stem cell.

of glomerular ultra-structural damage (**Figure 1H**), were highest in IR-SS and lowest in SC, significantly lower in IR-SS + Ex4 + ADMSC than in IR-SS + Ex4 and IR-SS + ADMSC, but they showed no difference between the latter two groups. Urine amount, an index of glomerular-filtration integrity, was highest in IR-SS + Ex4 + ADMSC and lowest in IR-SS, but was not different among the groups of SC, IR-SS + Ex4 and IR-SS + ADMSC (**Figure 1G**).

*Flow cytometric analysis of circulating level of inflammatory cells and mortality rate by day 3 after IR-SS procedure (**Figure 2**)*

The mortality rate from SC to IR-SS + Ex4-ADMSC was 0% (0/16), 56.25% (9/16), 31.25% (5/16), 37.5% (6/16) and 18.75% (3/16), respectively (**Figure 2A**). By Pairwise comparisons (without Bonferroni's correction), the mortality rate between two different groups was (1) SC vs. IR-SS, P=0.0004, (2) SC vs. IR-SS + Ex4, P=0.016, (3) SC vs. IR-SS + ADMSC, P=0.007, (4) SC vs. IR-SS + Ex4 + ADMSC, P=0.074, (5) IR-SS vs. IR-SS + Ex4 + ADMSC, P=0.015, (6) IR-SS vs. IR-SS + Ex4, P=0.156, (7) IR-SS vs. IR-SS + ADMSC, P=0.212, and (8) IR-SS + Ex4 vs. IR-SS + ADMSC, P=0.816, respectively (**Figure 2B**).

The circulating level of level Ly6G+ cells, an indicator of innate inflammatory reaction, was highest in in IR-SS and lowest in SC, significantly higher in IR-SS + Ex4 and IR-SS + ADMSC than that in IR-SS + Ex4 + ADMSC, and significantly higher in IR-SS + Ex4 than that in IR-SS + ADMSC (**Figure 2C**).

The circulating level of TLR-2 was significantly higher in IR-SS and lowest in SC and IR-SS + Ex4-ADMSC, and significantly in IR-SS + Ex4 than in IR-SS + ADMSC, but it showed no difference between SC and IR-SS + Ex4-ADMSC (**Figure 2D**).

The circulating levels of TLR-4 and CD14/TLR-2 were significantly higher in IR-SS than in other

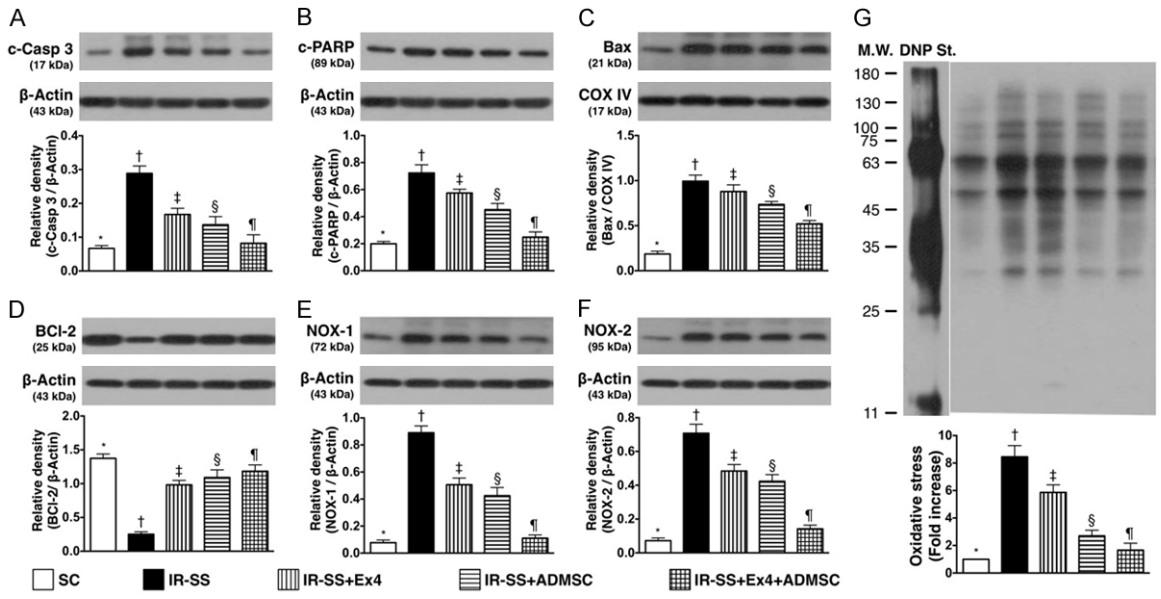


**Figure 5.** Protein expressions of apoptotic, anti-apoptotic and oxidative-stress biomarkers in kidney parenchyma by day 3 after IR-SS procedure. A. Protein expression of cleaved caspase 3 (c-Casp 3), * vs. other groups with different symbols (†, ‡, §, ¶), P<0.0001. B. Protein expression of cleaved Poly (ADP-ribose) polymerase (c-PARP), * vs. other groups with different symbols (†, ‡, §, ¶), P<0.0001. C. Protein expression of mitochondrial (mito)-Bax, * vs. other groups with different symbols (†, ‡, §, ¶), P<0.0001. D. Protein expression of Bcl-2, * vs. other groups with different symbols (†, ‡, §, ¶), P<0.0001. E. Protein expression of NOX-1, * vs. other groups with different symbols (†, ‡, §, ¶), P<0.0001. F. Protein expression of NOX-2, * vs. other groups with different symbols (†, ‡, §, ¶), P<0.0001. G. Oxidized protein expression, * vs. other groups with different symbols (†, ‡, §, ¶), P<0.0001. (Note: left and right lanes shown on the upper panel represent protein molecular weight marker and control oxidized molecular protein standard, respectively). M.W = molecular weight; DNP = 1-3 dinitrophenylhydrazone. All statistical analyses were performed by one-way ANOVA, followed by Bonferroni multiple comparison post hoc test (at least n=7 for each group). Symbols (*, †, ‡, §, ¶) indicate significance (at 0.05 level). SC = sham-operative control; IR-SS = ischemia-reperfusion and sepsis syndrome; Ex4 = exendin-4; ADMSC = adipose-derived mesenchymal stem cell.

groups and significantly higher in IR-SS + Ex4 than in SC, IR-SS + ADMSC and IR-SS + Ex4 + ADMSC, but it showed no difference among the later three groups (**Figure 2E**, **2F**). However, the circulating level of CD14/TLR-4 did not differ among the five groups (**Figure 2G**).

*Light microscopic findings for assessment of kidney injury score and small vessel density in kidney parenchyma by day 3 after IR-SS procedure (**Figure 3**)*

Light microscopy of H&E-stained kidney sections revealed that kidney injury score was highest in IR-SS and lowest in SC, significantly higher in IR-SS + Ex4 and IR-SS + ADMSC than that in IR-SS + Ex4 + ADMSC, and significantly higher in IR-SS + Ex4 than that in IR-SS + ADMSC (**Figure 3A-F**). On the other hand, α-smooth muscle actin staining for identifying vessel density in kidney parenchyma exhibited that the number of small vessels (i.e., the diameter ≤25 μM) exhibited an opposite pattern to kidney injury score among the five groups (**Figure 3G-L**).

*The protein expression of inflammatory and anti-inflammatory biomarkers in kidney parenchyma by day 3 after IR-SS procedure (**Figure 4**)*

The protein expressions of MMP-9, IL-1ß, TNF-α, TLR-2 and TLR-4, five indicators of inflammation, were highest in IR-SS, lowest in SC, and significantly higher in IR-SS + Ex4 than in IR-SS + ADMSC and IR-SS + Ex4 + ADMSC (**Figure 4A-E**). However, protein expressions of IL-4 and IL-10, two indices of anti-inflammation, showed progressive increases from SC to IR-SS + Ex4 + ADMSC, suggesting a phenomenon of intrinsic response to inflammatory stimulation (**Figure 4F**, **4G**).

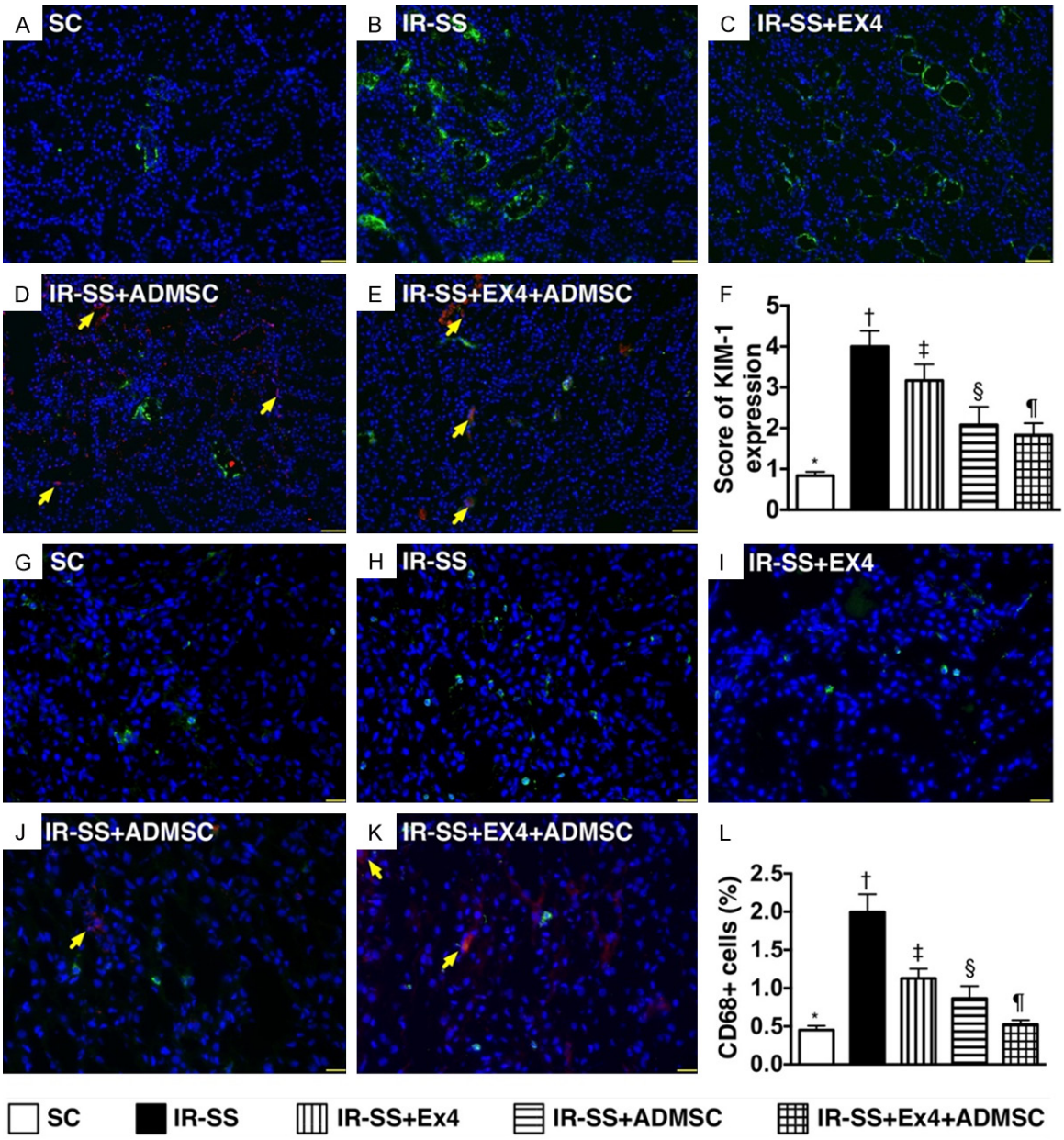


**Figure 6.** Kidney injury marker and inflammatory cells in kidney parenchyma by day 3 after IR-SS procedure. (A-E) Immunofluorescent (IF) microscopy (400 x) of kidney injury molecule (KIM)-1+ cells (green color). (F) Analytical result of number of KIM-1+ cells, * vs. other groups with different symbols (†, ‡, §, ¶), P<0.0001. (G-K) IF microscopy (400 x) of CD68+ cells (green color). (L) Analytical result of number of CD68+ cells, * vs. other groups with different symbols (†, ‡, §, ¶), P<0.0001. The blue color in the illustrating pictures indicated the DAPI stain for identification of nuclei. The red color with DiI stained nucleus (yellow arrows) in (D, E, J and K) indicated the dye-labeling ADMSCs. Scale bars in right lower corner represent 20 μm. All statistical analyses were performed by one-way ANOVA, followed by Bonferroni multiple comparison post hoc test (at least n=7 for each group). Symbols (*, †, ‡, §, ¶) indicate significance (at 0.05 level). SC = sham-operative control; IR-SS = ischemia-reperfusion and sepsis syndrome; Ex4 = exendin-4; ADMSC = adipose-derived mesenchymal stem cell.

*The protein expressions of apoptotic, anti-apoptotic and oxidative-stress biomarkers in kidney parenchyma by day 3 after IR-SS procedure (**Figure 5**)*

The protein expression of cleaved caspase 3, cleaved PARP and mitochondrial Bax, three indicators of apoptosis, were highest in IR-SS, lowest in SC, significantly higher in IR-SS + Ex4 and IR-SS + ADMSC than in IR-SS + Ex4 + ADMSC, and significantly higher in IR-SS + Ex4 than in IR-SS + ADMSC (**Figure 5A-C**). Conversely, the protein expression of Blc-2, an indicator of anti-apoptosis, showed an opposite pat-

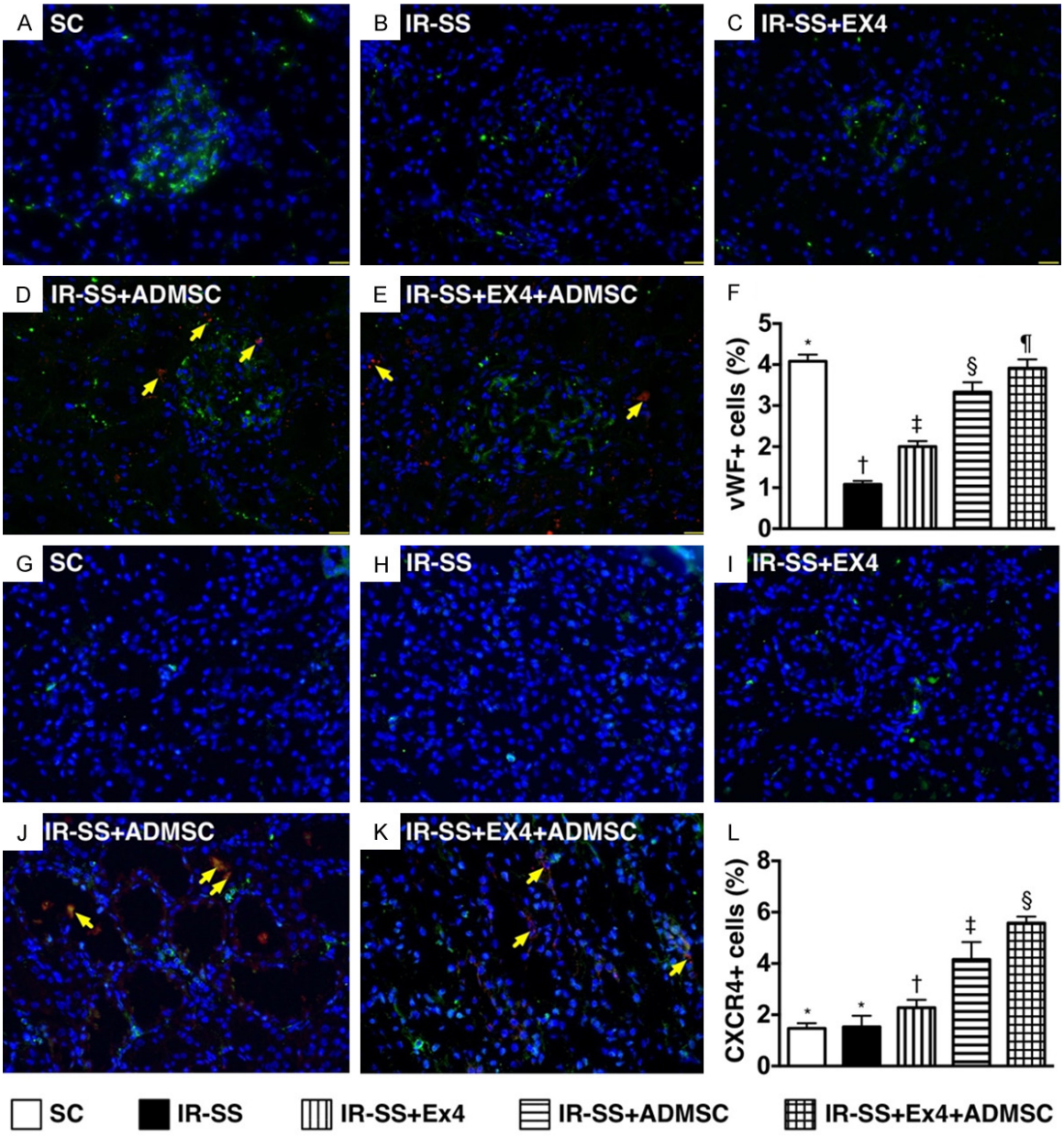


**Figure 7.** Cell angiogenesis in kidney parenchyma by day 3 after IR-SS procedure. (A-E) Immunofluorescent (IF) microscopy (400 x) for von Willebrand factor (vWF)+ cells in kidney parenchyma. (F) Analytical result of number of vWF+ cells, * vs. other groups with different symbols (†, ‡, §, ¶), P<0.0001. (G-K) The IF microscopy (100 x) of CXCR4+ cells in kidney parenchyma. (L) Analytical result of number of CXCR4+ cells, * vs. other groups with different symbols (†, ‡, §), P<0.0001. The blue color in the illustrating pictures indicated the DAPI stain for identification of nuclei. The red color with DiI stained nucleus (yellow arrows) in (D, E, J and K) indicated the dye-labeling ADMSCs. Scale bars in right lower corner represent 20 μm. All statistical analyses were performed by one-way ANOVA, followed by Bonferroni multiple comparison post hoc test (at least n=7 for each group). Symbols (*, †, ‡, §, ¶) indicate significance (at 0.05 level). SC = sham-operative control; IR-SS = ischemia-reperfusion and sepsis syndrome; Ex4 = exendin-4; ADMSC = adipose-derived mesenchymal stem cell.

tern to the apoptotic biomarkers among the five groups (**Figure 5D**).

The protein expressions of NOX-1, NOX-2 and oxidized protein, three indicators of oxidative stress, exhibited an identical pattern to apoptosis among the five groups (**Figure 5E-G**).

*Inflammatory cell infiltration and angiogenesis expressions in kidney parenchyma by day 3 after IR-SS procedure (**Figures 6, 7**)*

IF microscopic finding showed that the KIM-1, a kidney injury biomarker predominant expression in renal tubules, was highest in IR-SS, low-

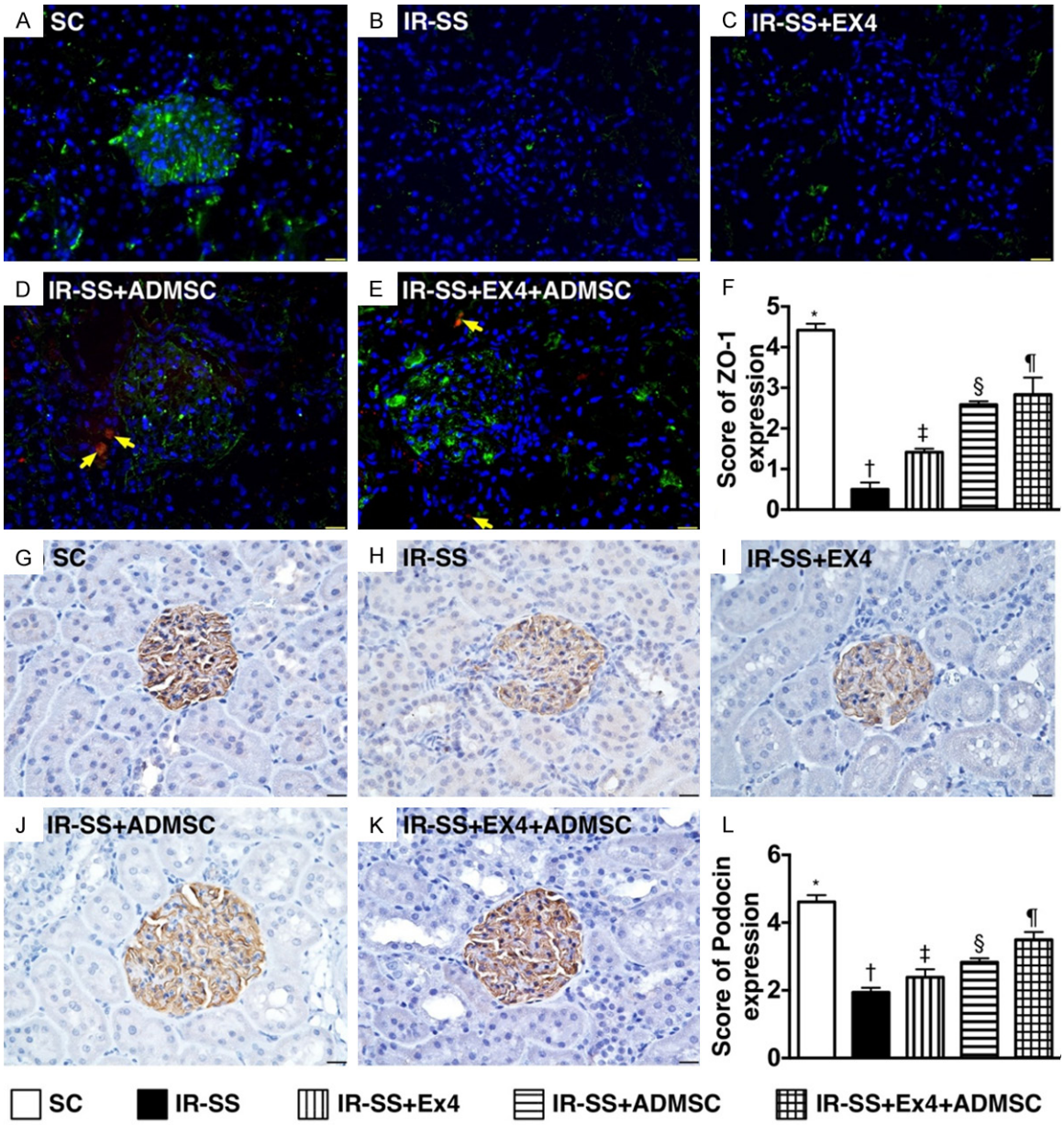


**Figure 8.** Assessment of ZO-1+ and podocin+ cells in kidney parenchyma by day 3 after IR-SS procedure. (A-E) Immunofluorescent microscopy (400 x) for ZO-1+ cells (green color) in kidney parenchyma. (F) Analytical result of number of ZO-1+ cells, * vs. other groups with different symbols (†, ‡, §, ¶), P<0.0001. The red color with Dil stained nucleus (yellow arrows) in (D) and (E) indicated the dye-labeling ADMSCs. (G-K) Immunohistochemical microscopy (400 x) for podocin+ cells (gray color) in kidney parenchyma. (L) Analytical result of number of podocin+ cells, * vs. other groups with different symbols (†, ‡, §, ¶), P<0.0001. Scale bars in right lower corner represent 20 μm. All statistical analyses were performed by one-way ANOVA, followed by Bonferroni multiple comparison post hoc test (at least n=7 for each group). Symbols (*, †, ‡, §, ¶) indicate significance (at 0.05 level). SC = sham-operative control; IR-SS = ischemia-reperfusion and sepsis syndrome; Ex4 = exendin-4; ADMSC = adipose-derived mesenchymal stem cell.

est in SC, significantly higher in IR-SS + Ex4 and IR-SS + ADMSC than in IR-SS + Ex4-ADMSC, and significantly higher in IR-SS + Ex4 than in IR-SS + ADMSC. (**Figure 6A-F**). Additionally, the IF microscopy demonstrated that the cellular expressions of CD68, an indicator of inflammation, displayed an identical pattern of KIM-1 among the five groups (**Figure 6G-L**).

IF microscopy also showed that the cellular expression of vWF (**Figure 7A-F**), an indicator of endothelial function, exhibited an opposite pat-

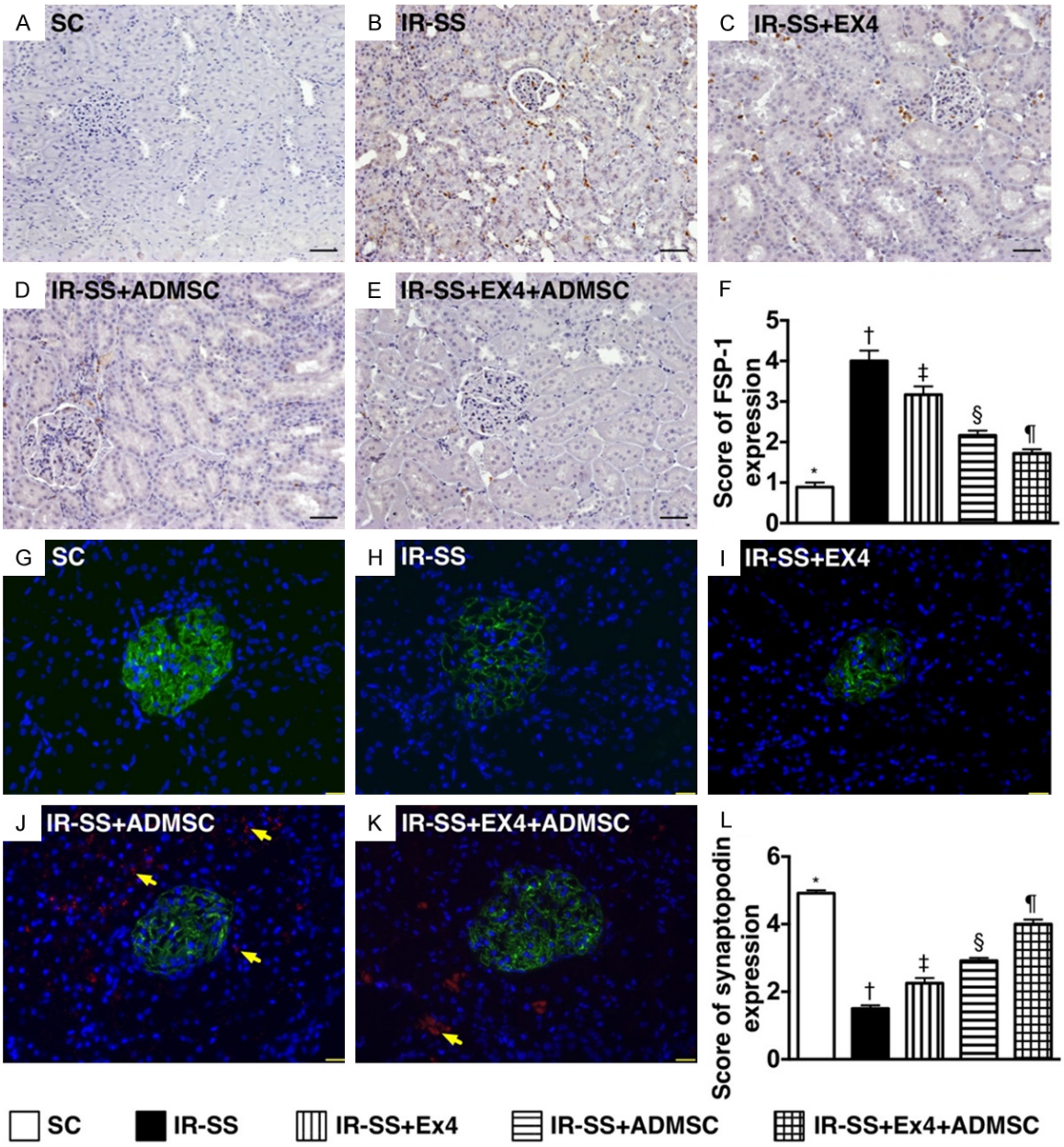


**Figure 9.** Assessment of FSP-1+ and synaptopodin+ cells in kidney parenchyma by day 3 after IR-SS procedure. (A-E) Immunofluorescent (IHC) microscopy (400 x) of fibroblast specific protein (FSP)-1+ cells (gray color) in kidney parenchyma. (F) Analytic result of number of FSP-1+ cells, * vs. other groups with different symbols (†, ‡, §, ¶), P<0.0001. (G-K) Immunofluorescent microscopy (400 x) for synaptopodin+ cells (green color) in kidney parenchyma. (L) Analytical result of number of synaptopodin+ cells, * vs. other groups with different symbols (†, ‡, §, ¶), P<0.0001. The red color with Dil stained nucleus (yellow arrows) in (J) and (K) indicated the dye-labeling ADMSCs. Scale bars in right lower corner represent 20 μm. All statistical analyses were performed by one-way ANOVA, followed by Bonferroni multiple comparison post hoc test (at least n=7 for each group). Symbols (*, †, ‡, §, ¶) indicate significance (at 0.05 level). SC = sham-operative control; IR-SS = ischemia-reperfusion and sepsis syndrome; Ex4 = exendin-4; ADMSC = adipose-derived mesenchymal stem cell.

tern to inflammatory cells among the five groups. On the other hand, the IF microscopy identified that the cellular expression of CXCR4, an indicator of endothelial progenitor cell/angiogenesis, significantly progressively increased from SC to IR-SS + Ex4-ADMSC (**Figure 7G-L**).

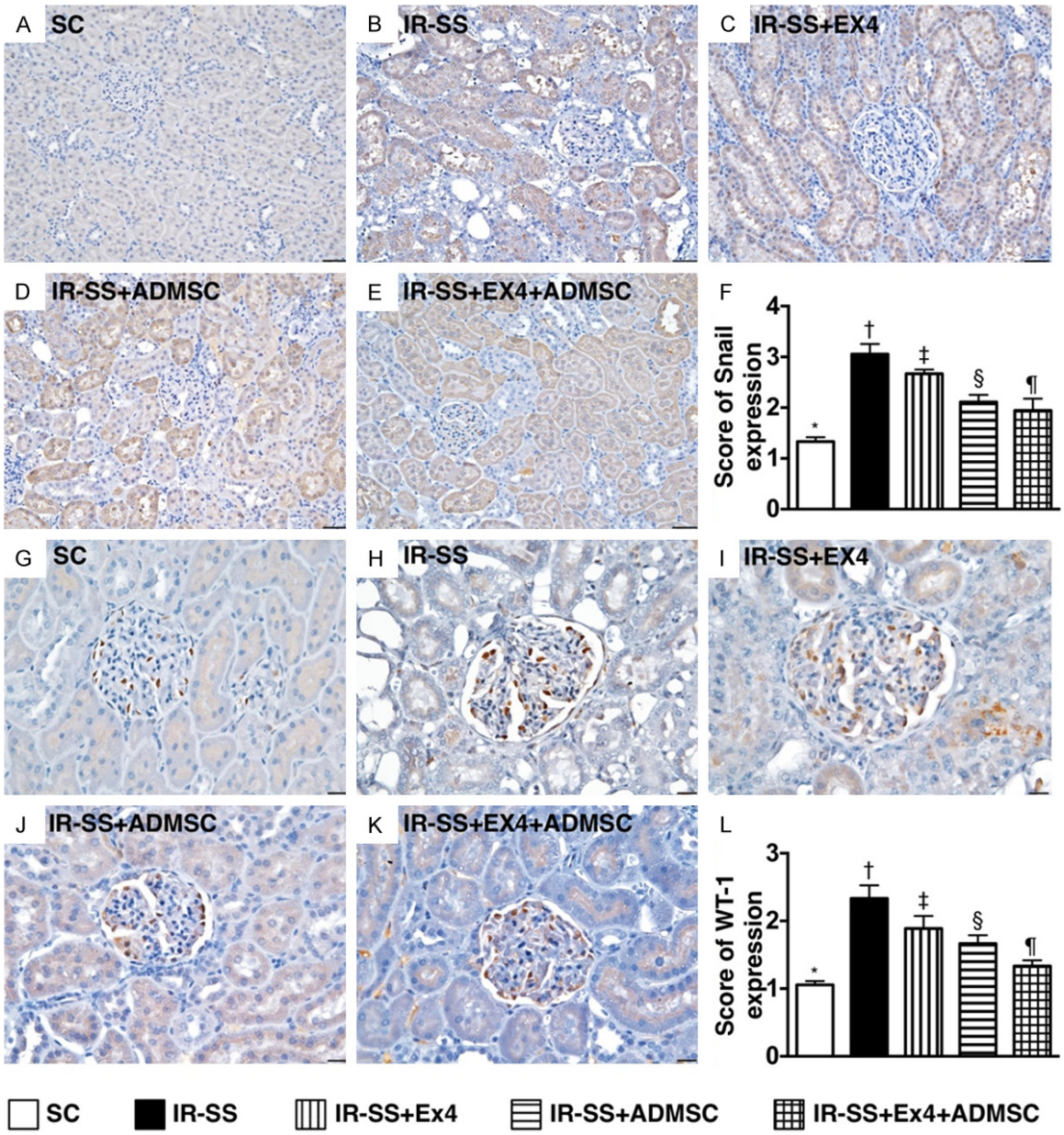


**Figure 10.** Identification of snail+ and WT-1+ cells in kidney parenchyma by day 3 after IR-SS procedure. (A-E) IHC immunohistochemical (IHC) microscopy (400 x) for snail+ cells (gray color) in kidney parenchyma. (F) Analytic result of number of snail-1+ cells, * vs. other groups with different symbols (†, ‡, §, ¶), P<0.0001. (G-K) IHC microscopy (400 x) for Wilm's tumor suppressor gene (WT)-1+ cells (gray color) in kidney parenchyma. (L) Analytic result of number of snail-1+ cells, * vs. other groups with different symbols (†, ‡, §, ¶), P<0.0001. Scale bars in right lower corner represent 20 μm. All statistical analyses were performed by one-way ANOVA, followed by Bonferroni multiple comparison post hoc test (at least n=7 for each group). Symbols (*, †, ‡, §, ¶) indicate significance (at 0.05 level). SC = sham-operative control; IR-SS = ischemia-reperfusion and sepsis syndrome; Ex4 = exendin-4; ADMSC = adipose-derived mesenchymal stem cell.

*Microscopic findings of podocyte components and renal tubules at day 3 after IR-SS procedure (**Figures 8-10**)*

IF analysis displayed that the expression of ZO-1, a tight junction-associated protein that offers a link between the integral membrane proteins and the filamentous cytoskeleton in podocytes, was highest in SC, lowest in IR-SS, significantly higher in IR-SS + Ex4-ADMSC than in IR-SS + Ex4 and IR-SS + ADMSC, and significantly higher in IR-SS + ADMSC than in IR-SS +

Ex4 (**Figure 8A-F**). Consistently, IHC staining showed that the expression of podocin, a component of podocyte foot process revealed an identical pattern to ZO-1 among the five groups (**Figure 8G-L**).

Additionally, IHC staining showed that changes in the expression of fibroblast specific protein 1 (FSP-1), which is mainly situated in kidney interstitials, showed an opposite pattern compared with ZO-1 among the five groups (**Figure 9A-F**). On the other hand, IF demonstrated that the synaptopodin, a podocyte foot process component, displayed an identical pattern to ZO-1 among the five groups (**Figure 9G-L**). Furthermore, IHC staining revealed that snail, predominantly accumulated in the tubular nuclei (**Figure 10A-F**), and WT-1, predominantly in podocytes (**Figure 10G-L**), showed an opposite pattern to ZO-1 among the five groups.

## Discussion

This study investigated the therapeutic effect of Ex4-ADMS in a preclinical setting of IR-SS and yielded several striking implications. First, the present study successfully created an experimental model that mimicked the clinical setting of AKI complicated by SS, which is an extremely common scenario in daily clinical practice. Additionally, based on this experimental model, we delineated that IR-SS damaged the kidney through highly complex pathomechanisms. Second, the histopathological findings (i.e., destructive glomerular and renal tubular architectures were identified by kidney injury score) explained why remarkably high urine protein to creatinine ratio and circulating levels of BUN and creatinine were found in animals with acute renal IR-SS compared to SC animals. Third, the results of the present study highlighted that Ex4-ADMSC therapy contributed a marked additive therapeutic effect for protecting kidney architecture (i.e., glomeruli and renal tubules) against IR-SS injury, inviting prospective clinical trials to evaluate the potential impact of this combined regimen in patients with AKI complicated by SS, especially DM patients.

An essential finding in the present study is that the circulating levels of BUN and creatinine, two important indices of AKI/renal dysfunction, were notably increased in animals with IR-SS at day 3 compared with sham-operated controls. Additionally, the ratio of urine protein to creatinine, another renal functional indicator, was comparable to that of creatinine level, whereas, the urine amount revealed an opposite pattern to creatinine level among the five groups; this indicates the fragility of kidney to damage in various disease entities, including IR-SS.

It is well recognized that AKI/acute kidney IR injury and IR-SS occur commonly in the clinical setting. Most previous studies [23, 25-28] utilized the experimental model of AKI/acute kidney IR injury rather than the experimental model of IR-SS to investigate the outcomes or effects of different management strategies. To the best of our knowledge, this is the first experimental model that mimicked the clinical setting of AKI/acute kidney IR injury complicated by SS. Importantly, the results of the present study demonstrated that combined treatment with Ex4 and ADMSC was superior to either alone for protecting kidney against IR-SS.

The inflammatory reaction and overwhelming immune response associated with generation of ROS/oxidative stress have been identified as the two processes with crucial roles for organ damage leading to inevitable functional deterioration and poor acute outcomes [9-13, 29]. Another essential finding in the present study was that the cellular and protein levels of inflammatory reactions were markedly upregulated in IR-SS animals compared to SC. In addition, the generation of ROS/oxidative stress was markedly augmented in an identical way between the two groups. These findings could partially explain why the renal function (i.e., increased circulating levels of creatinine and BUN) was remarkably impaired and the kidney architecture affected detrimentally (i.e., an increase in kidney injury score) in IR-SS animals. Importantly, these parameters in IR-SS animals were significantly reversed by Ex4 and ADMSC treatment and further significantly reversed after receiving Ex4-ADMSC treatment.

Previous [30-32] and our recent [15] studies have shown that the presence of intact podocytes and functional integrity between podocytes and their components (i.e., primary processes, secondary processes and foot processes) play major roles in establishing a size-selective barrier to protein loss. An important finding in the present study was that, when we looked at the cellular level of microscopic findings, the integrity [i.e., **Figures 8-10**] of ultrastructural components of podocytes was sub-

stantially devastated in IR-SS animals as compared with SC. Additionally, apoptotic biomarkers in kidney parenchyma were also substantially higher in IR-SS animals than in the SC. These molecular-cellular perturbations could explain why the ratio of urine protein to creatinine was remarkably increased in IR-SS animals compared to SC. As expected, these molecular-cellular perturbations in IR-SS animals were notably suppressed by Ex4 or ADMSC treatment and further suppressed by Ex4-ADMSC treatment.

Abundant data have shown that angiogenesis plays a crucial role in the restoration of blood flow to ischemic regions, to improve IR-caused/ischemia-related organ dysfunction [20, 21, 23-25, 33]. Stem cell therapy enhances angiogenesis, as has been clearly identified by copious previous studies [20, 21, 23-25, 33]. Furthermore, Ex4 has anti-oxidative stress effects as well as angiogenesis capacity through upregulating the circulating levels of endothelial progenitor cells, angiogenesis factors and vascular density in ischemic regions [14, 17]. A principal finding in the present study, at cellular and tissue levels, was that angiogenesis biomarkers as well as vessel density were significantly higher in IR-SS + Ex4 and in IR-SS + ADMSC animals, and even more significantly higher in IR-SS + Ex4 + ADMSC animals as compared to IR-SS animals. These findings reinforce previous studies [14, 17, 20, 21, 23-25, 33] and help explain why renal function and renal parenchyma were notably preserved in the former three groups of animals than in the latter group of animals.

## Study limitation

This study has limitations. First, the purpose of the study was designed to investigate the acute phase of IR-SS that mimicked daily clinical practice. Long-term outcomes from IR-SS were therefore out with the scope of this present study. Second, despite the extensive investigations in the present study, the precise mechanism of Ex4-ADMSC therapy that improves outcomes in rodents after IR-SS is still not entirely clear.

## Conclusion

In conclusion, the results of the present study demonstrated that Ex4-ADMSC therapy effectively protected the integrity of kidney parenchyma and renal function in the setting of IR-SS in rodents.

## Acknowledgements

This study was supported by a grant from Chang Gung Memorial Hospital, Chang Gung University (Grant number: CMRPG8E0281). All authors have read the journal's policy and declare no any potential conflicts of interest. Besides, this article has been reviewed by and approved by all named authors.

## Disclosure of conflict of interest

None.

## Authors' contribution

Pei-Hsun Sung and Hsin-Ju Chiang: design, data acquisition, analysis, and drafting the manuscript. Christopher Glenn Wallace, Chih-Chao Yang, Yen-Ta Chen, Kuan-Hung Chen, and Chih-Hung Chen: laboratory assay and troubleshooting. Pei-Lin Shao, Yung-Lung Chen, Sarah Chua, Han-Tan Chai, Yi-Ling Chen, and Tien-Hung Huang: data acquisition, analysis, and interpretation. Hon-Kan Yip and Mel S. Lee: conceived of the study, participated design, coordination, and helped to draft the manuscript.

## Abbreviations

Ex4, exendin-4; ADMSC, adipose-derived mesenchymal stem cell; IR, ischemia-reperfusion; SS, sepsis syndrome; AKI, acute kidney injury; RIFLE, Risk, Injury, Failure, Loss and End-stage; DM, diabetes mellitus; ROS, reactive oxygen species; GLP-1, glucagon-like peptide-1; MSC, mesenchymal stem cells; CLP, cecal ligation and puncture; Ly6G, Lymphocyte antigen 6 complex locus G6D; PBMC, peripheral blood mononuclear cell; TLR, toll-like receptor; BUN, blood urine nitrogen; ZO-1, zonula occludens-1; WT-1, Wilm's tumor suppressor gene 1; KIM-1, kidney injury molecule-1; vWF, Von Willebrand factor; CXCR4, C-X-C chemokine receptor type 4; FSP-1, fibroblast specific protein-1; MMP-9, matrix metalloproteinase-9; TNF-α, tumor necrosis factor-α; NF-κB, nuclear factor-κB; PARP, Poly-ADP-ribose polymerase; NOX, NADPH oxidase.

**Address correspondence to:** Dr. Mel S Lee, Department of Orthopedics, Kaohsiung Chang Gung Memorial Hospital, Chang Gung University College

of Medicine, 123, Dapi Road, Niaosung Dist., Kaohsiung 83301, Taiwan, R.O.C. Tel: +886-7-7317123; Fax: +886-7-7322402; E-mail: mellee@cgmh.org.tw; Dr. Hon-Kan Yip, Division of Cardiology, Department of Internal Medicine, Kaohsiung Chang Gung Memorial Hospital and Chang Gung University College of Medicine, 123, Dapi Road, Niaosung Dist., Kaohsiung 83301, Taiwan, R.O.C. Tel: +886-7-7317123; Fax: +886-7-7322402; E-mail: han.gung@msa.hinet.net

## References

[1] Groeneveld AB, Tran DD, van der Meulen J, Nauta JJ and Thijs LG. Acute renal failure in the medical intensive care unit: predisposing, complicating factors and outcome. Nephron 1991; 59: 602-610.

[2] Pickering JW, James MT and Palmer SC. Acute kidney injury and prognosis after cardiopulmonary bypass: a meta-analysis of cohort studies. Am J Kidney Dis 2015; 65: 283-293.

[3] Thongprayoon C, Cheungpasitporn W, Srivali N, Ungprasert P, Kittanamongkolchai W, Greason KL and Kashani KB. Acute kidney injury after transcatheter aortic valve replacement: a systematic review and meta-analysis. Am J Nephrol 2015; 41: 372-382.

[4] Coca SG, Yusuf B, Shlipak MG, Garg AX and Parikh CR. Long-term risk of mortality and other adverse outcomes after acute kidney injury: a systematic review and meta-analysis. Am J Kidney Dis 2009; 53: 961-973.

[5] Ricci Z, Cruz DN and Ronco C. Classification and staging of acute kidney injury: beyond the RIFLE and AKIN criteria. Nat Rev Nephrol 2011; 7: 201-208.

[6] Kim WY, Huh JW, Lim CM, Koh Y and Hong SB. A comparison of acute kidney injury classifications in patients with severe sepsis and septic shock. Am J Med Sci 2012; 344: 350-356.

[7] Kim WY, Huh JW, Lim CM, Koh Y and Hong SB. Analysis of progression in risk, injury, failure, loss, and end-stage renal disease classification on outcome in patients with severe sepsis and septic shock. J Crit Care 2012; 27: 104, e101-107.

[8] Ratanarat R, Skulratanasak P, Tangkawattanakul N and Hantaweepant C. Clinical accuracy of RIFLE and acute kidney injury network (AKIN) criteria for predicting hospital mortality in critically ill patients with multi-organ dysfunction syndrome. J Med Assoc Thai 2013; 96 Suppl 2: S224-231.

[9] Bilgili B, Haliloglu M and Cinel I. Sepsis and acute kidney injury. Turk J Anaesthesiol Reanim 2014; 42: 294-301.

[10] Vincent JL. Acute kidney injury, acute lung injury and septic shock: how does mortality compare? Contrib Nephrol 2011; 174: 71-77.

[11] Goncalves GM, Zamboni DS and Camara NO. The role of innate immunity in septic acute kidney injuries. Shock 2010; 34 Suppl 1: 22-26.

[12] Aziz M, Jacob A, Yang WL, Matsuda A and Wang P. Current trends in inflammatory and immunomodulatory mediators in sepsis. J Leukoc Biol 2013; 93: 329-342.

[13] Sung PH, Chiang HJ, Chen CH, Chen YL, Huang TH, Zhen YY, Chang MW, Liu CF, Chung SY, Chen YL, Chai HT, Sun CK and Yip HK. Combined therapy with adipose-derived mesenchymal stem cells and ciprofloxacin against acute urogenital organ damage in rat sepsis syndrome induced by intrapelvic injection of cecal bacteria. Stem Cells Transl Med 2016; 5: 782-792.

[14] Sheu JJ, Chang MW, Wallace CG, Chiang HJ, Sung PH, Tsai TH, Chung SY, Chen YL, Chua S, Chang HW, Sun CK, Lee FY and Yip HK. Exendin-4 protected against critical limb ischemia in obese mice. Am J Transl Res 2015; 7: 445-459.

[15] Yip HK, Yang CC, Chen KH, Huang TH, Chen YL, Zhen YY, Sung PH, Chiang HJ, Sheu JJ, Chang CL, Chen CH, Chang HW and Chen YT. Combined melatonin and exendin-4 therapy preserves renal ultrastructural integrity after ischemia-reperfusion injury in the male rat. J Pineal Res 2015; 59: 434-447.

[16] Lu HI, Chung SY, Chen YL, Huang TH, Zhen YY, Liu CF, Chang MW, Chen YL, Sheu JJ, Chua S, Yip HK and Lee FY. Exendin-4 therapy still offered an additional benefit on reducing transverse aortic constriction-induced cardiac hypertrophy-caused myocardial damage in DPP-4 deficient rats. Am J Transl Res 2016; 8: 778-798.

[17] Chua S, Lee FY, Chiang HJ, Chen KH, Lu HI, Chen YT, Yang CC, Lin KC, Chen YL, Kao GS, Chen CH, Chang HW and Yip HK. The cardioprotective effect of melatonin and exendin-4 treatment in a rat model of cardiorenal syndrome. J Pineal Res 2016; 61: 438-456.

[18] Oeseburg H, de Boer RA, Buikema H, van der Harst P, van Gilst WH and Sillje HH. Glucagon-like peptide 1 prevents reactive oxygen species-induced endothelial cell senescence through the activation of protein kinase A. Arterioscler Thromb Vasc Biol 2010; 30: 1407-1414.

[19] Kim S, Moon M and Park S. Exendin-4 protects dopaminergic neurons by inhibition of microglial activation and matrix metalloproteinase-3 expression in an animal model of Parkinson's disease. J Endocrinol 2009; 202: 431-439.

[20] Sun CK, Leu S, Hsu SY, Zhen YY, Chang LT, Tsai CY, Chen YL, Chen YT, Tsai TH, Lee FY, Sheu JJ, Chang HW and Yip HK. Mixed serum-deprived and normal adipose-derived mesenchymal stem cells against acute lung ischemia-reper-

fusion injury in rats. Am J Transl Res 2015; 7: 209-231.
[21] Chang CL, Sung PH, Sun CK, Chen CH, Chiang HJ, Huang TH, Chen YL, Zhen YY, Chai HT, Chung SY, Tong MS, Chang HW, Chen HH and Yip HK. Protective effect of melatonin-supported adipose-derived mesenchymal stem cells against small bowel ischemia-reperfusion injury in rat. J Pineal Res 2015; 59: 206-220.
[22] Ko SF, Yip HK, Zhen YY, Lee CC, Lee CC, Huang CC, Ng SH and Lin JW. Adipose-derived mesenchymal stem cell exosomes suppress hepatocellular carcinoma growth in a rat model: apparent diffusion coefficient, natural killer T-cell responses, and histopathological features. Stem Cells Int 2015; 2015: 853506.
[23] Lin KC, Yip HK, Shao PL, Wu SC, Chen KH, Chen YT, Yang CC, Sun CK, Kao GS, Chen SY, Chai HT, Chang CL, Chen CH and Lee MS. Combination of adipose-derived mesenchymal stem cells (ADMSC) and ADMSC-derived exosomes for protecting kidney from acute ischemia-reperfusion injury. Int J Cardiol 2016; 216: 173-185.
[24] Chen KH, Chen CH, Wallace CG, Yuen CM, Kao GS, Chen YL, Shao PL, Chen YL, Chai HT, Lin KC, Liu CF, Chang HW, Lee MS and Yip HK. Intravenous administration of xenogenic adipose-derived mesenchymal stem cells (ADMSC) and ADMSC-derived exosomes markedly reduced brain infarct volume and preserved neurological function in rat after acute ischemic stroke. Oncotarget 2016; 7: 74537-74556.
[25] Chen HH, Lin KC, Wallace CG, Chen YT, Yang CC, Leu S, Chen YC, Sun CK, Tsai TH, Chen YL, Chung SY, Chang CL and Yip HK. Additional benefit of combined therapy with melatonin and apoptotic adipose-derived mesenchymal stem cell against sepsis-induced kidney injury. J Pineal Res 2014; 57: 16-32.
[26] Chen YT, Tsai TH, Yang CC, Sun CK, Chang LT, Chen HH, Chang CL, Sung PH, Zhen YY, Leu S, Chang HW, Chen YL and Yip HK. Exendin-4 and sitagliptin protect kidney from ischemia-reperfusion injury through suppressing oxidative stress and inflammatory reaction. J Transl Med 2013; 11: 270.
[27] Urbschat A, Zacharowski K, Obermuller N, Rupprecht K, Penzkofer D, Jennewein C, Tran N, Scheller B, Dimmeler S and Paulus P. The small fibrinopeptide Bbeta15-42 as renoprotective agent preserving the endothelial and vascular integrity in early ischemia reperfusion injury in the mouse kidney. PLoS One 2014; 9: e84432.
[28] Chang MW, Chen CH, Chen YC, Wu YC, Zhen YY, Leu S, Tsai TH, Ko SF, Sung PH, Yang CC, Chiang HJ, Chang HW, Chen YT and Yip HK. Sitagliptin protects rat kidneys from acute ischemia-reperfusion injury via upregulation of GLP-1 and GLP-1 receptors. Acta Pharmacol Sin 2015; 36: 119-130.
[29] Chang CL, Leu S, Sung HC, Zhen YY, Cho CL, Chen A, Tsai TH, Chung SY, Chai HT, Sun CK, Yen CH and Yip HK. Impact of apoptotic adipose-derived mesenchymal stem cells on attenuating organ damage and reducing mortality in rat sepsis syndrome induced by cecal puncture and ligation. J Transl Med 2012; 10: 244.
[30] Drenckhahn D and Franke RP. Ultrastructural organization of contractile and cytoskeletal proteins in glomerular podocytes of chicken, rat, and man. Lab Invest 1988; 59: 673-682.
[31] Bariety J, Nochy D, Mandet C, Jacquot C, Glotz D and Meyrier A. Podocytes undergo phenotypic changes and express macrophagic-associated markers in idiopathic collapsing glomerulopathy. Kidney Int 1998; 53: 918-925.
[32] Barisoni L, Mokrzycki M, Sablay L, Nagata M, Yamase H and Mundel P. Podocyte cell cycle regulation and proliferation in collapsing glomerulopathies. Kidney Int 2000; 58: 137-143.
[33] Chen YL, Tsai TH, Wallace CG, Chen YL, Huang TH, Sung PH, Yuen CM, Sun CK, Lin KC, Chai HT, Sheu JJ, Lee FY and Yip HK. Intra-carotid arterial administration of autologous peripheral blood-derived endothelial progenitor cells improves acute ischemic stroke neurological outcomes in rats. Int J Cardiol 2015; 201: 668-683.